Manuscript for Kidney International

Association between Randall's plaque and calcifying nanoparticles

NEVA ÇİFTÇİOĞLU, PhD[1,4], KAVEH VEJDANI, MD[2], OLIVIA LEE MD[2], GRACE MATHEW, MS[1,4], KATJA M. AHO, MS[3], E. OLAVI KAJANDER, MD, PhD[4], DAVID S. McKAY, PhD[5], JEFF A. JONES, MD, PhD[5], MATTHEW HAYAT, PhD[6], and MARSHALL L. STOLLER*****, MD[2]

[1]Nanobac Pharmaceuticals, Johnson Space Center, Houston, TX/USA, [2]Department of Urology, University of California at San Francisco, San Francisco, CA/USA, [3]University of Kuopio, Department of Biosciences/Biochemistry, Kuopio/Finland, [4]Nanobac Pharmaceuticals, Tampa, FL/USA, [5]National Aeronautics and Space Administration, Johnson Space Center, Houston, TX/USA, [6]Universities Space Research Association, Johnson Space Center, Houston, TX/USA

* Corresponding author
Marshall Stoller [mstoller@urology.ucsf.edu]

Contact person:
NEVA ÇİFTÇİOĞLU
Address: Nanobac Pharmaceuticals Inc., Johnson Space Center, 2101 NASA Parkway, Mail code KA, Houston / TX
Tel: 281-483-7198
Fax: 281-483-1573
Email: Neva.Ciftcioglu-1@nasa.gov

Key words: Calcifying nanoparticles, nanobacteria, Randall's plaque, urinary stone

Running headline: renal papilla and calcifying nanoparticles

Acknowledgement
This research was funded by ARES/Astrobiology at NASA Johnson Space Center (JSC), and Nanobac Pharmaceuticals Inc. We thank Dr. Adam Hittelman at University of California at San Francisco (UCSF) for coordinating patients' serum and tissue samples, Dr. Craig Schwandt (NASA, JSC) for his support in electron microscopy, and Dr. Jean Olson (UCSF) for her assistance in evaluating immunohistochemistry interpretaton. Special thanks to Mission Pharmacal for providing discussion points on stone formation. Our gratitude to Dr. Dan Garrison (NASA JSC) for his efficient management of BSL-2 laboratories and Charles Galindo (NASA, JSC) for his assistance. Patrice Colbert's (NASA, JSC) proficiency in editing the text is greatly appreciated.

Abstract

Background. Randall's plaques, first described by Alexander Randall in the 1930s, are small subepithelial calcifications in the renal papillae (RP) that also extend deeply into the renal medulla. Despite the strong correlation between the presence of these plaques and the formation of renal stones, the precise origin and pathogenesis of Randall's plaque formation remain elusive. The discovery of calcifying nanoparticles (CNP) and their detection in many calcifying processes of human tissues has raised hypotheses about their possible involvement in renal stone formation.

Methods. We collected RP and blood samples from 17 human patients who had undergone laparoscopic nephrectomy due to neoplasia. Homogenized RP tissues and serum samples were cultured for CNP. Scanning electron microscopy (SEM) and energy dispersive X-ray spectroscopy (EDS) analysis were performed on fixed RP samples. Immunohistochemical staining (IHS) was applied on the tissue samples using CNP-specific monoclonal antibody (mAb).

Results. Randall's plaques were visible on gross inspection in 11 out of 17 collected samples. Cultures of all serum samples and 13 tissue homogenates had CNP growth within 4 weeks. SEM revealed spherical apatite formations in 14 samples, with calcium and phosphate peaks detected by EDS analysis. IHS was positive in 9 out of 17 samples.

Conclusion. A strong link was found between the presence of Randall's plaques and the detection of CNP, also referred to as nanobacteria. These results suggest new insights into the etiology of Randall's plaque formation, and will help us understand the pathogenesis of stone formation. Further studies on this topic may lead us to new approaches on early diagnosis and novel medical therapies of kidney stone formation.

Introduction

Over 65 years ago, Randall performed a detailed examination of the kidney papillae of more than 1,000 nonselected cadaveric renal units, and demonstrated that interstitial crystals located at, or adjacent to, the papillary tip were common in stone formers [1]. He found that these crystals were composed not of calcium oxalate (CaOx), the most common solid phase found in patients with nephrolithiasis, but of calcium phosphate (CaP) [2], and termed them as plaques. He believed that the CaP crystals precipitated in the papillary interstitium and subsequently eroded into the urinary space, serving as a nucleation surface for CaOx [2]. *In vitro*, CaP phases such as apatite efficiently nucleate CaOx crystallization [3], so that one can easily conjecture that common CaOx stones begin on plaques. Most theories, including that of Randall, have held as axiomatic that particle retention must be a prerequisite to stone formation [4]. Finlayson later argued that, due to rapid flow of the renal ultrafiltrate through the tubule, there was insufficient time for formation of an inralumenal-obstructing solid phase [5], which also suggested that an intratubular site of stone formation was unlikely. However, other investigators found that CaOx crystals adhered to cultured tubular cells [6], where they could either be endocytosed or remain on the cell surface, serving as a nidus for growth into larger, clinically significant, calculi.

In addition to studies of the initiation mechanism of kidney stone formation, other nephrolithiasis factors were examined. Between 1980 and 1994 the prevalence of kidney stone disease increased by 37% for unknown reasons [7]. In the field of infectious diseases, increasing disease rate has been accepted as a possible indicator of infectious

agent involvement. For example, a significant increase in stomach ulcer incidence was eventually correlated with presence of *Helicobacter pylori* infection and subsequent studies showed that most stomach ulcers are directly caused by this infection [8].

Calcifying nanoparticles (CNP), also referred to as nanobacteria, were discovered over a decade ago in blood and blood products [9, 10] and correlated with numerous pathological-calcification related diseases such as prostatitis [11, 12], arteriosclerosis [13-16], malignant tumors [17, 18], Alzheimer's disease [19], gall stones [20], calciphylaxis [21, 22] and polycystic kidney disease [23, 24]. It also has been hypothesized that CNP are the initial nidi on which kidney stones develop at a rate dependent on the degree of supersaturation of the urine [25-28]. The basic CNP are membrane-enclosed cell-like vesicles that are 100 times smaller in volume than common bacteria [10]. These units contain no detectable genomic DNA or RNA, but yet appear capable of self propagation or replication [29]. We have explored the possibility that such particles could be primitive life forms [30]. Although we know their capability of causing specific infection [31], general debate continues over the systematic classification of these particles among infectious agents. Methods to detect CNP in biological samples, cells, tissues, and blood include immuno-detection techniques using anti-CNP mAbs, specific culture techniques and electron microscopy [32]. With the help of those developed methodologies, some important features of CNP and their triggering effect on nephrolithiasis have been suggested by different research teams. These features include:

1. CNP consist of tiny spheres (50-200nm) resembling cells or liposomes. They appear to readily precipitate apatite from their surrounding media forming apatite-protein complexes. Immuno-electronmicroscopy reveals protein antigens in close

proximity to precipitated apatite, suggesting a novel form of protein-associated mineralization [33].

2. This mineralization starts as extremely small apatite crystals and forms on the exterior membrane of 50-200nm diameter CNP followed by a growing shell or an enclosing sphere of apatite which may reach a diameter of one to several micrometers [34, 35].
3. 14% of healthy adults in Scandinavia have anti-CNP antibodies [36]. A high fraction (75%) of patient groups with kidney diseases has CNP antigen [37].
4. CNP form apatite units/shells *in vitro,* morphologically and chemically similar to those in the core of kidney stones, see Figure 1. [24, 25].
5. CNP are renotropic [38].
6. CNP cause kidney stone formation when injected into rats via percutaneous renal puncture [39].
7. CNP have been detected in many different types of human kidney stones [25, 28].
8. In laboratory experiments, destruction of the calcified apatite shell of CNP with EDTA-chelation reveals numerous 50 to 100nm diameter membranous cells [34] similar to those observed in Randall plaques by other research groups [4, 40-42].
9. Transmission Electron Microscopy (TEM) study of renal plaques shows 1-5 μm apatite spheres laminated with mineral and organic molecules [4, 41, 42], similar to the structure of CNP shells [10, 27], see Figure 2.

Matlaga, et al in their recent review article stated that in the decades since Randall first reported his observations there has been little progress in defining the role of plaque in the pathogenesis of kidney stone diseases, fundamentally due to lack of appropriate *in*

vivo data [4]. Our goal was to test the hypothesis of CNP-Randall's plaque association by obtaining RP samples from patients whose kidneys have been removed due to neoplasia. We present here preliminary evidence that there is a strong association between Randall's plaques and CNP.

Materials and Methods

Subjects

RP were dissected from 17 patients who had undergone laparoscopic nephrectomy due to neoplasia. Presence or absence of Randall's plaques were noted on gross inspection of immediately extracted and bivalved kidneys. Selected papillae were harvested well away from the tumor. Tissue samples were prepared for the analyses with SEM, EDS, IHS, and CNP culture. Blood was drawn in the fasting state from each patient immediately before and after surgery. The serum was extracted and used for CNP culture and enzyme-linked immunosorbent assay (ELISA) to detect CNP antigen and antibody. A bladder urine sample of each patient was drawn through a urinary catheter and sent for routine urine culture. The study was approved by the UCSF Committee on Human Research and every patient was given detailed information regarding the procedures involved in this research and signed an informed consent prior to any manipulation.

Tissue preparation for analysis

RP specimens of 17 patients for IHC and SEM experiments were immediately immersed in 4% paraformaldehyde and refrigerated overnight. IHS samples were paraffin

embedded and prepared for IHS as described earlier [43]. SEM samples were dehydrated and gold-coated as described previously [10]. The tissue samples for CNP cultures were immediately placed into 2 ml of sterile phosphate buffered saline (PBS), pH 7.4, homogenized for 30 seconds, four times, with 30-second cooling intervals on ice using conventional, 5-ml glass tissue-grinders. Homogenized tissue was centrifuged at 2500g for 15 minutes. The supernatant was separated under sterile conditions and sterile-filtered through 0.22μm pore size, non-protein binding filters (Millipore) into sterile non-adhesive tubes and stored at -70^{o}C until thawed and processed for culture as described below.

CNP cultures from serum and tissue samples

Patient serum samples, and homogenized tissue supernatant samples were cultured in Dulbecco's Modified Eagle's Medium (DMEM, Gibco Lab Inc., Grand Island, NY) under mammalian cell culture conditions (37^{o}C, 5-10% CO_2, 90-95 % humidity) for four weeks. Patient sera were cultured at 10% final concentration, and tissue homogenates were cultured both with and without fetal bovine serum (FBS) supplementation which was previously tested for CNP and evaluated as CNP negative (Atlanta Biologicals, GA) as described earlier [44]. The pellets from the homogenized tissue were incubated with 30 mM EDTA for 1 hour at room temperature for decalcification, and release of enclosed CNP from the apatite units, diluted 1:10 in DMEM, and cultured as described above. Each sample was filtered through 0.22 μm filters before culturing in order to eliminate potential conventional-bacterial contamination in a Biosafety level-2 facility. Cultures were checked for gross bacterial contamination by microscopy and macroscopic

observation of turbidity and color change of the medium from the third day of incubation. Control culture plates were incubated in parallel with the test plates to determine whether spontaneous crystallization can occur in culture medium. The medium was incubated with or without FBS. Every week, the culture plates were inspected by phase contrast microscopy (Nikon Eclipse TE 2000-U) for CNP growth. Positive identification of CNP involved typical slow propagation and optical properties, negative signal with Hoechst 33258 dye, and positive signal with indirect immunofluorescence staining (IIFS) [10]. All culture samples were harvested with 14000g centrifugation for 30 min at 4^{o}C followed by 30 days of incubation. The pellets were spread on glass slides for IIFS, fixed and double-stained using CNP surface-antigen-specific mAb 8D10 (Nanobac Oy, Kuopio, Finland), followed by Alexa Fluor 488 goat-anti-mouse IgG [32]. In addition, Hoechst stain was used to detect conventional bacterial contamination. As a positive control for Hoechst, *E. coli* (nonpathogenic strain HB101) was used. Fluorescence photographs were taken using an Olympus BX60F5 microscope coupled to a Nikon digital camera DXM 1200F.

Scanning electron microscopy and energy dispersive X-ray microanalysis

RP samples 2-4 mm in block size were analyzed both for morphology and chemical composition using JEOL 6340 Field Emission SEM with attached IXRF EDS analyzer [10]. Each sample was divided into 4 mapping areas and each area was scanned for small, 100-500 nm spherical forms, and apatite, calcium-rich or phosphate-rich particles. Cultured CNP and one oxalate kidney stone (gift from University of Kuopio Hospital/Finland) sample were prepared for SEM analysis using the same preparation

technique for tissue samples. In EDS analyses, inorganic hydroxyapatite (Sigma, H-0252, St. Louis, MO) was used as a reference.

Immunohistochemical analysis of renal papilla samples

Paraffin embedded RP tissue samples were cut into 5-μm sections, deparaffinized and rehydrated [43]. Each tissue section was demineralized in 250 mM sodium citrate for 24 hours at +4^{o}C, to retrieve apatite crystal-covered epitopes prior to IHS. After washing in water, endogenous peroxidase was blocked with 1% H_2O_2 in methanol for 30 min. Slides were then rinsed in PBS before staining with a catalyzed Signal Amplification (CSA) IHS (Dako, Carpinteria, CA, USA). Anti-CNP mAb, 8D10, was used as primary antibody which is recommended by the manufacturer for detection of CNP in formalin-fixed paraffin embedded tissue sections. All slides were counterstained with hematoxylin, and mounted with glycerol. Negative control sections went through the same staining process, except that the primary mAb step was omitted.

Biochemical Assays

All blood specimens were obtained in the early morning and after an overnight fast, before and after surgery. Serum samples were prepared within 2 hours and kept frozen at -70^{o}C until analyzed. The commercially available ELISA kits for detecting anti-CNP IgG and CNP antigen; Nano-Sero IgG, and Nanocapture (Nanobac Oy, Finland) respectively were used. All measurements were run in duplicates.

Nano-Sero IgG ELISA measures quantitatively a cumulative immune reaction to the antigen complex in special conformation on CNP, and includes for instance heterophilic

antibodies and auto-antibodies. Nanocapture ELISA measures quantitatively CNP from a 50µl serum sample. The detection antibody recognizes CaP-binding protein-antigen on CNP in a special CaP complex conformation (ELISA kit inserts).

Statistical analysis

Tissue samples for 17 patients were analyzed with several techniques and measurements in the form of a rating recorded. The serum and tissue homogenate cultures for CNP had a rating of (4)= growth in one week, (3)= growth in two weeks, (2)= growth in three weeks, (1)= growth in four weeks, (0)= no growth in four weeks of incubation. SEM was rated as (0) if no CNP was observed, (1) if CNP were seen in one of the four mapped areas, (2) if CNP were seen two of the four mapped area, (3) if CNP were seen three of the four mapped area, and (4) if CNP were seen in every scanned area at 1500X magnification. The Nanocapture and Nano-sero ELISA performed on 16 patient sera, and values obtained for CNP antigen and antibody tests were evaluated as follows: for Nanocapture ELISA: (0) indicates < 3.5 units/ml; (1) > 3.5-11.0 units/ml; (2) > 11.0-50.0 units/ml; (3) > 50.0-150 units/ml; (4) > 150 units/ml. For Nano-sero ELISA: (0) indicated < 0.1 units/ml; (1) > 0.1 - 0.4 units/ml; (2) > 0.4 - 0.5 units/ml; (3) > 0.5 - 0.7 units/ml; (4) > 0.7 units/ml.

While no control subjects were observed in this study, historical data from our other CNP-related experiments on healthy subjects is available [36] and discussed further in the Discussion. Summary tables were used to describe the ratings taken and a logistic regression model with a random effect for subject was used to test for agreement between the tissue-tests performed when ratings are categorized as a positive or negative result.

Results

Subjects

Eleven male and 6 female patients were enrolled in our study, with a mean age of 65.5 and 78 years, respectively. Randall's plaques were observed on the RP of 11 patients (Table 1), with no sexual preponderance. No correlation was found between the observation of Randall's plaques and the patients' tumor types or their past medical histories. Urine cultures were negative in 12 patients, showed mild growth of genital flora in 3 patients and were positive for enterococcus species in 2 patients.

CNP cultures of serum samples and tissue homogenates

All serum samples and 13 of 17 RP tissue homogenates and tissue pellets grew CNP at different growth rates (Tables 1 and 2). Some samples were already positive within three days of culture. All growth-positive samples stained positive with IIFS using anti-CNP mAb, 8D10 (Fig. 3A), but stained negative with the Hoechst (Fig. 3B), indicating no bacterial contamination in cultures. The positive control for Hoechst dye, *E. coli,* was stained blue (Fig. 3C), but no signal was detected with 8D10 (Fig. 3D). Electron microscopic observation of cultured CNP showed typical morphology of CNP (Fig 4A), but no protein precipitation or inorganic type crystal formation was observed as we have described the comparisons of those particular morphologies earlier [26, 29]. In negative controls, no CNP growth, no mineralization or protein precipitation was observed during the one-month follow-up.

Scanning Electron Microscopic Analysis

Fourteen of 17 tissue samples contained CNP shell-like particles in variable sizes (Fig. 4 B-D and Fig 5B) which also produced CaP peaks under EDS analysis identical to that of CNP (Fig 5C). The tissue samples without visible, macroscopic plaques had fewer or no spherical apatite formations compared with samples with visible plaques (Figure 6). The tissue cells with those apatite particles looked more deformed with fibrous formation (Figs. 4 C, D and 6F) whereas the negative tissue cells looked more intact with a healthy tissue appearance (Figs. 5A and 6G). The apatite spheres produced an EDS pattern (Fig. 5C) identical to the CNP EDS patterns as observed in our earlier studies [10, 25, 26].

Immunohistochemistry

The results of RP samples analyzed using IHS is summarized in Table 1. Nine out of 17 tissue samples stained positive for CNP antigen. Positive staining results as a brown-colored precipitate at the antigen site is shown in Fig.7 A, B and F. Negative controls that were stained with the same technique by omitting the mAb, did not show any non-specific brown staining (Fig 7 E).

ELISA

Out of 16 tested serum samples, 14 were positive for CNP-antigen, and 11 were positive for CNP-antibody. Nano-Sero IgG, and Nanocapture ELISA test results are summarized at Tables 1 and 2.

Statistical Results

Ratings in the experiment results were categorized into positive and negative groups, and results of a logistic regression model with a random effect for subject yield a p-value of p=0.2427 for the statistical test of an overall difference between tissue sample tests. The results for the serum culture for CNP were excluded from this statistical test since all subjects recorded a positive rating. Thus there is a lack of evidence for rejecting the null hypothesis of a difference between the results of the seven tissue sample tests and we can conclude that the tissue sample test results did not differ for the different techniques used.

Discussion

Plaques, defined as sites of interstitial crystal deposition at or near the papilla tip, are found in kidneys of CaOx-stone formers (100%) and often, but less frequently, in people who do not form CaOx stones (43%) [45]. Stoller and colleagues used high-resolution radiography to examine 50 consecutive sets of cadaveric kidneys [46]. Renal medullary calcification that extended deep into papillae was identified in 57%. When histologically examined, the calcification was localized to the basement membrane of collecting tubules and vesa recta, as well as within the papillary interstitium. One major question is to determine how plaques themselves form, on what structures, and in response to what driving forces? Until the studies by Evan et al. [47, 48], we did not have an answer to these rather elementary questions. These investigators performed kidney biopsies on stone-forming patients to determine the anatomical site and composition of the initial solid phase. In calcium oxalate stone formers, they found initial CaP (apatite) crystallization in the basement membrane of the thin limbs of the loop of Henle with

subsequent extension to the vasa recta, then to the interstitial tissue surrounding the terminal collecting ducts, and finally, in the most severe cases, to the papillae. Contact of these crystals with urine, supersaturated with respect to calcium oxalate, may have promoted heterogeneous nucleation and formation of kidney stones. Non-stone formers, subjected to nephrectomy had neither plaque nor crystals [47-49].

Now that we know where the initial solid phase forms, and the potential metabolic factors provoking the stone formation, what are the next questions? The common paradigm is that the cores of kidney stones are made of apatite. Randall described papillary calculi as formations characteristically having a smooth convex surface and a concave surface, which he believed to be the site of papillary implantation [1, 2]. Why there was a common morphology in these formations if they were simple crystal depositions, and the reason of apatite crystal accumulation in the first place always remained elusive.

The discovery of CNP encapsulated in a CaP shell, and their subsequent detection in several human pathologic calcification processes, raised hopes for an explanation for Randall's plaques [34]. Soon after their discovery, the CNP were detected in urinary stones recovered from human patients [25, 28]. Inspired by these observations, we hypothesized that CNP might actually be the initiating agents in the formation of Randall's plaques and subsequently the renal stones.

Matlaga et al have used high power imaging, micro fourier transformed microspectroscopy, electron diffraction analysis on Randall's plaques and concluded that they are formed of spherical, biological apatite particles [4]. Those are very similar in morphology and composition to cultured shells of CNP (Figs 1B, 4A) [10, 25-27]. In our

earlier TEM analysis of CNP shells we defined their morphology as "tree-age-ring-like" formations of crystal and organic matter [27], a description which is almost identical to Coe et al's [41], and Matlaga et al's [4] observations in Randall's plaques (Fig. 2). We also have observed apatite spherical formations in the core of every kidney stone independent of their overall chemical composition of the kidney stones (Fig. 1) and cultured CNP from those stones [25]. Other independent studies also support our hypothesis that CNP may instigate kidney stone nucleation and growth [28, 34, 50-53].

The other research strengthening our hypothesis shows that bone-associated proteins, including osteopontin (OPN), bone morphogenetic protein 2 (BMP-2), alkaline phosphatase, matrix Gla protein, osteocalcin, bone sialoprotein, urinary prothrombin fragment 1 and type 1 collagen, have a role in plaque formation [54-58]. Kumar et al hypothesized that renal cells in culture can assume an osteoblast-like phenotype, express the matrix proteins OPN and BMP, and form calcified nodules [34]. These studies provide support for the hypothesis that renal cells may promote the formation of Randall's plaques, perhaps via expression of matrix proteins. Kajander et al described similar calcification promoting proteins on the surface of CNP (unpublished data).

CNP have unique properties including extremely small "cell" size (0.1-0.5 μm), and rapid *in situ* precipitation of CaP from blood and other body fluids under conditions not normally conducive to such precipitation [10]. The "cells" and associated apatite surfaces may act like a magnet to bind those kinds of proteins from the blood circulation, and enhancing calcification in the cells where they are attached and/or internalized. CNP are renotropic, as reported from rabbit experiments using radiolabelled CNP and are eliminated from the circulation through urinary excretion [38]. In another study, it was

shown that translumbar, percutaneous intrarenal injection of CNP into rats resulted in kidney stone formation [39]. In our earlier experiments, we have infected rats with IV CNP and observed strongly positive IHS results with specific CNP mAb especially localized at kidney glomerulus [24]. In this research, we appreciate similar findings with the renal plaque positive patients samples (Fig. 7A, B). Whether CNP themselves serve as the nucleus for crystal formation, or they are simply able to lower the activation energy barrier and thus allow precipitation and growth of crystals under much lower supersaturation conditions is yet to be determined. For evaluating the results of this study, it is immaterial whether or not CNP are even actual life forms or located into a certain category in Bergey's Manual, or some kind of vesicles or liposomes; their properties of promoting rapid crystallization and growth of calcium rich minerals are well established, and their involvement in other pathological calcification related diseases have been studied [24-27, 29].

Nephrolithiasis is a significant urological disease afflicting a large percentage of US population costing approximately 2.39 billion dollars per year [4]. Initial diagnosis of a kidney stone is frequently acute in onset, and commonly requires a variety of interventions. To reduce the likelihood of recurrence, it is necessary to understand the mechanisms involved in stone formation and to determine urinary markers of stone initiation. Earlier it was thought that knowing the site of initial crystallization would improve our understanding of the pathogenesis of stone formation and allow investigators to propose more focused hypotheses. This would help devise effective therapies aimed at preventing recurrent nephrolithiasis, which afflicts approximately 50% of stone formers within five years of the initial stone [59]. However, if there is an unknown causative

agent, the treatment approach will remain non-specific, palliative, and eventually ineffective, while the root cause remains unsolved. To a great extent, our studies accord with and confirm much of Randall's pioneering work. Plaque is interstitial and composed of apatite. What we add, here, is that the apatite formations are culturable, stainable with CNP-specific monoclonal antibodies, and the formation of nuclei or nidi apatite precipitates seems to be controlled by CNP. This important finding needs to be confirmed with a research design including a larger patient population and negative controls. We have developed diagnostic tools for this unique agent, and also found that CNP are susceptible to certain antibiotics [60]. If supported by further work, this hypothesis may lead to treatment designed to disable the CNP, prevent or control the precipitation of apatite, and treat the formation of kidney stones as a consequence of an infection.

Conclusion

We found a strong association between Randall's plaque of human kidneys, and the presence of CNP. While the results reported in this preliminary research are limited with only 17 patient samples and there are no plaque-negative renal samples involved, the presented hypothesis is critical and opens further discussions in the urology arena.

References

1. Randall A. The origin and growth of renal calculi. *Ann. Surg*. 105:1009-1027, 1937
2. Randall A. Papillary pathology as precursor of primary renal calculus. *J. Urol.* 44:580-589, 1940
3. Mandel GS, Mandel NS. 1996. Crystal-crystal interactions, in *Kidney stones: medical and surgical management*, edited by Coe FL, Favus MJ, Pak CYC, Parks JH, Preminger GM, Lippincott-Raven Publishers, Philadelphia, Pennsylvania, USA 1996, pp 115–128
4. Matlaga BR, Coe FL, Evan AP, Lingeman JE. The role of Randall's plaques in the pathogenesis of calcium stones. *J Urol.* 177:31-38, 2007
5. Finlayson B, Reid F. The expectation of free and fixed particles in urinary stone disease. *Invest. Urol*. 15:442-448, 1978
6. Lieske JC, Toback FG. Renal cell-urinary crystal interactions. *Curr. Opin. Nephrol. Hypertens.* 9:349-355, 2000
7. Stamatelou KK, Francis ME, Jones CA, Nyberg NM Jr, Curhan GC. Time trends in reported prevalence of kidney stones in the United States: 1976–1994. *Kid. Int.* 63 :1817–1823, 2003
8. Deeks JJ, Banatvala N. Helicobacter pylori: populations and cohorts. *J Infect Dis.* Dec;170(6):1634-1636, 1994
9. Çiftçioglu N, Kuronen I, Åkerman K, Hiltunen E, Laukkanen J, Kajander EO. A new potential threat in antigen and antibody products: Nanobacteria, in *Vaccines*

97 edited by Brown F, Burton D, Doherty P, Mekalanos J, Norrby E. Cold Spring Harbor Laboratory Press, Cold Spring Harbor, USA 1997, pp 99-103

10. Kajander EO, Çiftçioglu N. Nanobacteria: An alternative mechanism for pathogenic intra- and extracellular calcification and stone formation. *Proc. Natl. Acad. Sci. USA* 95:8274-8279, 1998
11. Wood HM, Shoskes DA. The role of nanobacteria in urologic disease. *World J Urol* 24:51-54, 2006
12. Shoskes DA, Thomas KD, Gomez E. Anti-nanobacterial therapy for men with chronic prostatitis/chronic pelvic pain syndrome and prostatic stones: preliminary experience. *J Urol* 173:474-477, 2005
13. Miller VM, Rodgers G, Charlesworth JA, et al. Evidence of nanobacterial-like structures in calcified human arteries and cardiac valves. *Am J Physiol Heart Circ Physiol* 287:1115-1124, 2004
14. Puskas LG, Tiszlavicz L, Razga Z, et al. Detection of nanobacteria-like particles in human atherosclerotic plaques. *Acta Biol Hung* 56:233-245, 2005
15. Jelic TM, Chang HH, Roque R, Malas AM, Warren SG, Sommer AP. Nanobacteria-associated calcific aortic valve stenosis. *J Heart Valve Dis.* Jan;16(1):101-5, 2007
16. Çiftçioğlu N, McKay DS, Kajander EO. Nanobacteria might be one of the potential agents in Oral Flora Triggering Peripheral Arterial Diseases. *Circulation* 108:58-59, 2003

17. Hudelist G, Singer CF, Kubista E, et al. Presence of nanobacteria in psammoma bodies of ovarian cancer: evidence for pathogenetic role in intratumoral biomineralization. *Histopathology* 45:633-637, 2004
18. Wainwright M. Nanobacteria and associated 'elementary bodies' in human disease and cancer. *Microbiology* 145:2623-2624, 1999
19. Kajander EO, Liesi P, Çiftçioglu N. Do Autonomously replicating sterile-filterable particles have an association with amyloid accumulation? *Viruses and virus-like agents in disease*. 2nd Karger Symposium, Basel, Switzerland, 1993, Abstract book, p41.
20. Wen Y, Li YG, Yang ZL, et al. Detection of nanobacteria in serum, bile and gallbladder mucosa of patients with cholecystolithiasis. *Chin Med J*, 118:421-424, 2005
21. Jelic TM, Malas AM, Groves SS, et al. Nanobacteria-caused mitral valve calciphylaxis in a man with diabetic renal failure. *South Med J*; 97:194-198, 2004
22. Lopez-Brea M, Selgas R. Nanobacteria as a cause of renal diseases and vascular calcifying pathology in renal patients ("endovascular lithiasis"). *Enferm Infec Microbiol Clin* 18:491-492, 2000
23. Hjelle JT, Miller-Hjelle MA, Poxton IR, et al. Endotoxin and nanobacteria in polycystic kidney disease. *Kidney Int*, 57:2360-2374, 2000
24. Kajander EO, Çiftçioğlu N, Miller-Hjelle MA, et al. Nanobacteria: controversial pathogens in nephrolithiasis and polycystic kidney disease. *Cur Opin Nephrol Hyperten*, 10:445-452, 2001

25. Çiftçioglu N, Björklund M, Willman K, Kuorikoski K, Bergström K, Kajander EO. Nanobacteria: an infectious cause for kidney stone formation. *Kidney International,* 56:1893-1898, 1999

26. Çiftçioglu N, Haddad RS, Golden DC, Morrison DR, McKay DS. Potential cause for kidney stone formation during space flights: enhanced growth of nanobacteria in microgravity. *Kidney Int.* 67:483-491, 2005

27. Kajander EO, Çiftçioglu N, Aho K, Garcia-Cuerpo E. Characteristics of nanobacteria and their possible role in stone formation. *Urol Res* 31:47-54, 2003

28. Shiekh FA, Khullar M, Singh SK. Lithogenesis: induction of renal calcifications by nanobacteria. *Urol Res* 34:53-57, 2006

29. Çiftçioglu N, McKay DS, Mathew G, Kajander EO. Nanobacteria: fact or fiction? Characteristics, detection, and medical importance of novel self-replicating, calcifying nanoparticles. *Journal of Investigative Medicine* 54:385-394, 2006

30. Kajander EO, Çiftçioğlu N. Nanobacteria as extremophiles, in *Instruments, Methods, and Missions for Astrobiology II,* edited by Richard B. Hoover Denver, The International Society for Optical Engineering, Proceedings of SPIE, 1999 3755 : 106-112

31. Çiftçioğlu N, Aho KM, McKay DS, Kajander EO. Are Apatite Nanoparticles Safe? *The Lancet* (in press).

32. Miller-Hjelle MA, Hjelle JT, N. Çiftçioğlu, and E. Olavi Kajander. Nanobacteria: Methods for growth and identification of this recently discovered calciferous agent, in *Rapid Analytical Microbiology. The Chemistry and Physics of Microbial*

Identification edited by, Wayne P. Olson, PDA Bethesda, MD, USA, Davis Horwood International Publishing, Ltd, Godalming. Surrey, 2003, UK. pp 297-312

33. Vali H, McKee MD, Çiftçioğlu N, Sears SK, Plows FL, Chevet E, Ghiasi P, Plavsic M, Kajander EO, Zare RN. Nanoforms: A new type of protein-associated Mineralization. *Geoch. Cosmoch. Acta.*, 65: 63-74, 2001
34. Kumar V, Farell G, Yu S, Harrington S, Fitzpatrick L, Rzewuska E, Miller VM, Lieske JC. Cell biology of pathologic renal calcification: contribution of crystal transcytosis, cell-mediated calcification, and nanoparticles. *J Investig Med*. 54:412-424, 2006
35. Benzerara K, Miller VM, Barell G, Kumar V, Miot J, Brown GE Jr, Lieske JC. Search for microbial signatures within human and microbial calcifications using soft x-ray spectromicroscopy. *J Investig Med.* 54:367-379, 2006
36. Holmberg M. Prevalence of Human Anti-Nanobacteria Antibodies Suggest Possible Zoonosis. 1st International Minisymposium on Nanobacteria, Kuopio, Finland, 2001, (http://www.nanobac.fi/nbminisymp080301/page10.html)
37. Hjelle JT, Miller-Hjelle MA, Poxton IR, Kajander EO, Çiftçioglu N, Jones ML, Caughey RC, Brown R, Millikin PD, Darras FS. Endotoxin and nanobacteria in polycystic kidney disease. *Kidney International*, 57: 2360-2374, 2000
38. Åkerman KK, Kuikka JT, Çiftçioglu N, Parkkinen J, Bergström KA, Kuronen I, Kajander EO. Radiolabeling and *in vivo* distribution of nanobacteria in rabbit, in *Instruments, Methods, and Missions for Astrobiology*, edited by Richard B.

Hoover, The International Society for Optical Engineering, Proceedings of SPIE, 3111: 436-442, 1997

39. García Cuerpo E, Kajander EO, Çiftçioğlu N, Castellano FL, Correa C, Gonzales J, Mampaso F, Liano F, De Gabiola ED, Berrilero YAE. Nanobacteria ; Un modelo de neo-litogenesis experimental. *Arch. Esp. de Urol* 53: 291-303, 2000
40. Williams JC Jr, Matlaga BR, Kim SC, Jackson ME, Sommer AJ, McAteer JA, Lingeman JE, Evan AP. Calcium oxalate calculi found attached to the renal papilla: Preliminary evidence for early mechanisms in stone formation. *J Endourol.* 20:885-890, 2006
41. Coe FL, Evan A, Worcester E. Kidney stone disease *The Journal of Clinical Investigation* 115: 2598-2608, 2005
42. Evan AP, Coe FL, Lingeman JE, Worcester E. Insights on the pathology of kidney stone formation. *Urol Res.* 33:383-389, 2005
43. Scheffer GL, Hu X, Pijnenborg AC, Wijnholds J, Bergen AA, Scheper RJ. MRP6 (ABCC6) detection in normal human tissues and tumors. *Lab Invest.* 82:515-518, 2002
44. Çiftçioglu N, Kajander EO. Interaction of Nanobacteria with cultured mammalian cells. *Pathophysiology* 4: 259-270, 1998
45. Low, RK, Stoller ML. Endoscopic mapping of renal papillae for Randall's plaques in patients with urinary stone disease. *J. Urol.* 158:2062-2064, 1997
46. Stoller ML, Shami GS, McCormick VD, Kerschmann RL. High resolution radiography of cadaveric kidneys: unraveling the mystery of Randall's plaque formation. *J. Urol.* 156:1263-1266, 1996

47. Evan AP, Coe FL, Lingeman JE, Worcester E. Insights on the pathology of kidney stone formation. *Urol Res*. 33:383-389, 2005

48. Evan A, Lingeman J, Coe FL, Worcester E. Randall's plaque: pathogenesis and role in calcium oxalate nephrolithiasis. *Kidney Int.* 69:1313-1318, 2006

49. Evan AP, Lingeman JE, Coe FL, Parks JH, Bledsoe SB, Shao Y, Sommer AJ, Paterson RF, Kuo RL, Grynpas M. Randall's plaque of patients with nephrolithiasis begins in basement membranes of thin loops of Henle. *J Clin Invest.* 111:602-605, 2003

50. Wood HM, Shoskes DA. The role of nanobacteria in urologic disease. *World J Urol.* 24:51-54, 2006

51. Conte Visús A, Grases Freixedas F, Costa-Bauzá A, Pizá Reus P. Microinfections and kidney lithiasis. *Arch Esp Urol.* 54:855-860, 2001

52. Goldfarb DS. Microorganisms and calcium oxalate stone disease. *Nephron Physiol.* 98:48-54 2004

53. López-Brea M, Selgas R. Nanobacteria as a cause of renal diseases and vascular calcifying pathology in renal patients ("endovascular lithiasis"). *Enferm Infecc Microbiol Clin.* 18:491-492, 2000

54. Hess B, Nakagawa Y, Coe FL. Inhibition of calcium oxalate monohydrate crystal aggregation by urine proteins. *Am J Physiol.* 257:99-106. 1989

55. Grover PK, Moritz RL, Simpson RJ, Ryall RL. Inhibition of growth and aggregation of calcium oxalate crystals in vitro--a comparison of four human proteins. *Eur J Biochem.* 253:637-644, 1998

56. Asplin JR, Arsenault D, Parks JH, Coe FL, Hoyer JR. Contribution of human uropontin to inhibition of calcium oxalate crystallization. *Kidney Int.* 53:194-199, 1998

57. Enghild JJ, Thøgersen IB, Cheng F, Fransson LA, Roepstorff P, Rahbek-Nielsen H. Organization of the inter-alpha-inhibitor heavy chains on the chondroitin sulfate originating from Ser(10) of bikunin: posttranslational modification of IalphaI-derived bikunin. *Biochemistry*. 38:11804-11813 1999

58. Stapleton AM, Ryall RL. Crystal matrix protein--getting blood out of a stone. *Miner Electrolyte Metab* 20:399-409, 1994

59. Asplin JR, Favus MJ, Coe FL. Nephrolithiasis, in *The kidney* edited by Brenner BM, Saunders WB. Company. Philadelphia, Pennsylvania, USA. 2000, pp. 1774–1819

60. Çiftçioğlu N, Miller-Hjelle MA, Hjelle JT, Kajander EO. Inhibition of nanobacteria by antimicrobial drugs as measured by modified microdilution method. *Antimicrob Agents Chemother* 46:2077-2086, 2002

Table 1. Overall Results for Tissue Sample Tests.

Result	**Observed Presence of Randall's plaques**	**Serum culture for CNP**	**Tissue homogenate culture for CNP**	**SEM**	**EDS**	**IH**	**ELISA Ag***	**ELISA Ab***
Negative	6	0	4	3	3	8	2	5
Positive	11	17	13	14	14	9	14	11

* Missing response for Subject 17

Table 2: Ratings for CNP, SEM, and ELISA Tissue Sample Tests.

Rating	Serum culture for CNP	Tissue homogenate culture for CNP	SEM	ELISA Ag*	ELISA Ab*
0	0	4	3	2	5
1	7	7	3	3	10
2	2	5	2	5	1
3	5	1	7	2	1
4	3	0	2	4	0

* Missing response for Subject 17

Figures

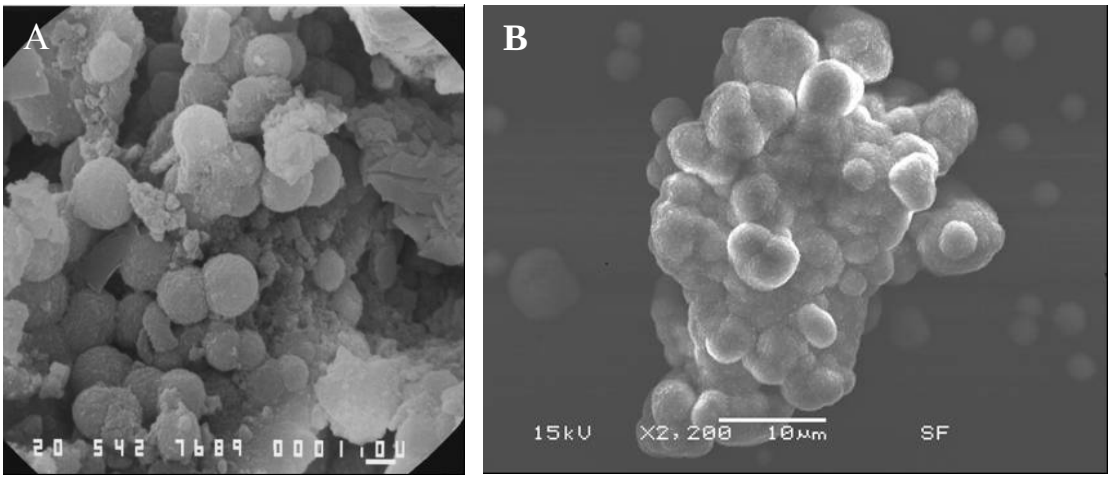

Figure 1. SEM images of apatite spheres in various sizes in the core of an oxalate kidney stone (A), apatite formations in the CNP culture (B). Bars= A; 1µm, B; 10µm.

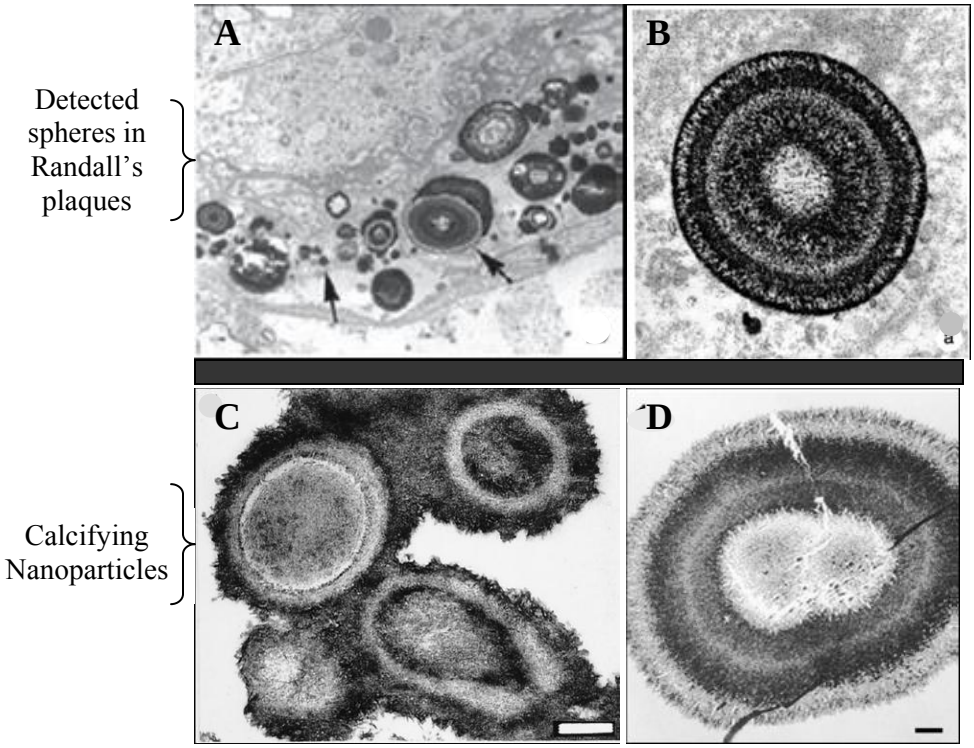

Figure 2. Morphological similarities of published TEM images of spherical, apatite containing formations in renal papilla (A and B), and CNP (C and D). Magnifications: A, 20,000X; B 30,000X; C and D, bars 200nm.

Reprinted from; A: Coe FL, Evan A, Worcester E. Kidney stone disease. *J Clin Invest*. 115:2598-2608, 2005 [41] with permission from American Urological Association. B: Matlaga BR, Coe FL, Evan AP, Lingeman JE. The role of Randall's plaques in the pathogenesis of calcium stones. *J Urol*. 177:31-38, 2007 [4] with permission from American Urological Association. C: Kajander EO, Ciftcioglu N. Nanobacteria: an alternative mechanism for pathogenic intra- and extracellular calcification and stone formation. *Proc Natl Acad Sci U S A*. 95:8274-8279, 1998 [10] with permission from copyright 1998 National Academy of Sciences USA. D: Kajander EO, Ciftcioglu N, Aho K, Garcia-Cuerpo E. Characteristics of nanobacteria and their possible role in stone formation. *Urol Res.* 31:47-54, 2003 [27] with kind permission from Springer Science and Business Media.

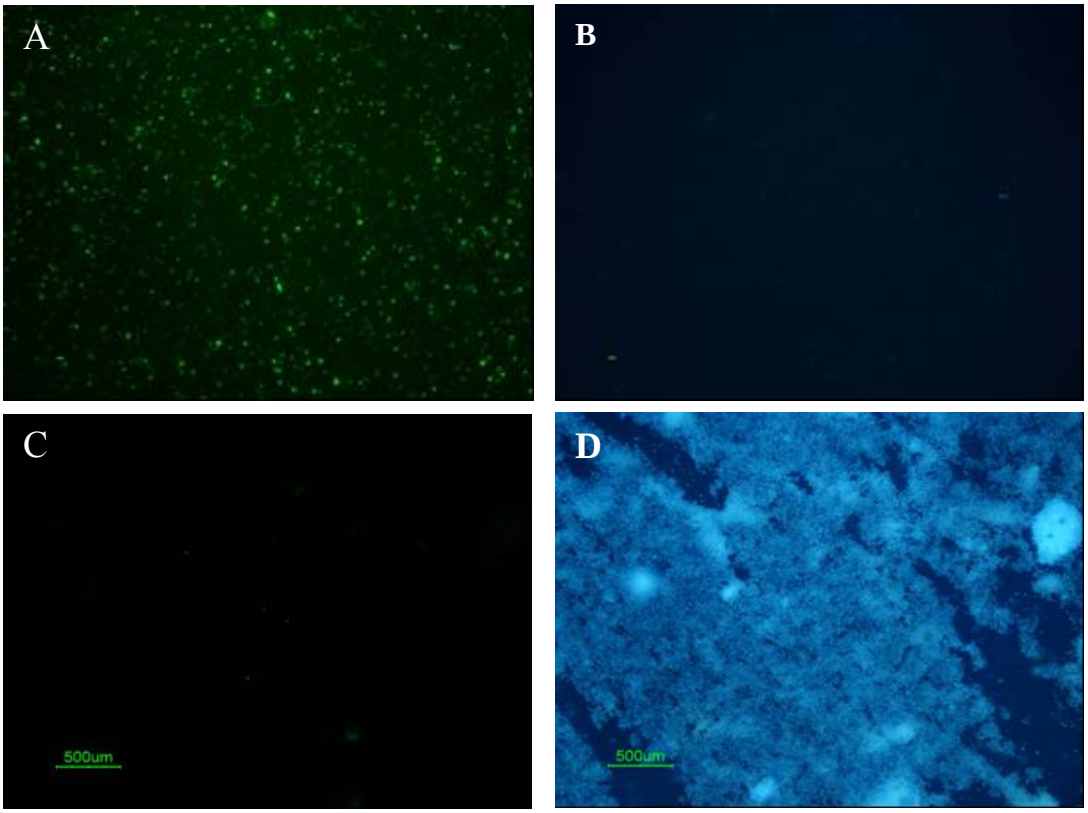

Figure 3. Light microscopic images of double staining results of patient samples cultured under CNP culture conditions. (**A)** IIFS positive cultured patient sample recognizing the CNP specific monoclonal antibody when imaged with the green bandpass emission filter, (**B)** Negative results of Hoechst die the same sample (A) imaged with the blue bandpass emission filter. (C) IIFS negative bacterial control (nonpathogenic *E. coli* strain HB101) not recognizing the CNP specific monoclonal antibody with green bandpass emission filter. (D) Positive results of Hoechst die the same sample (C) imaged with the blue bandpass emission filter.

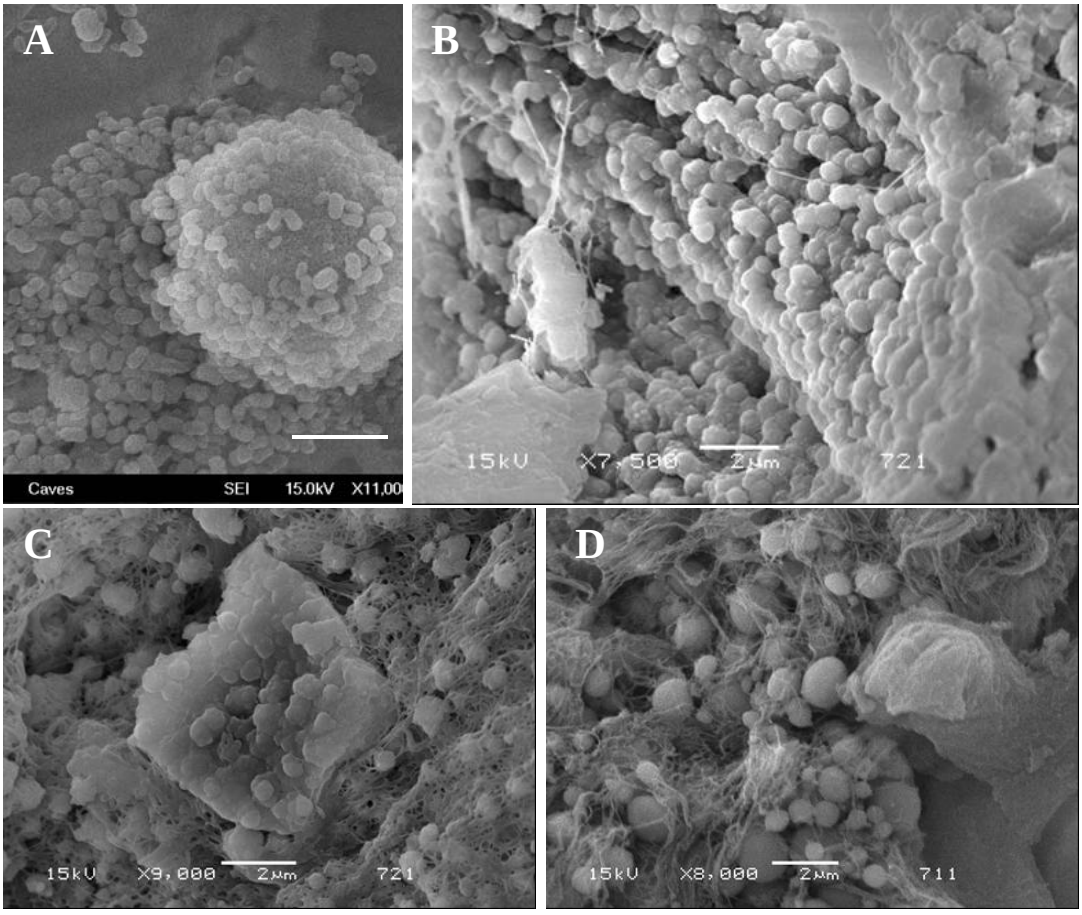

Figure 4. SEM images of (A): cultured CNP from a serum sample, (B, C, and D) CaP spheres detected on renal papilla (Randall's plaque). Bars; 2µm.

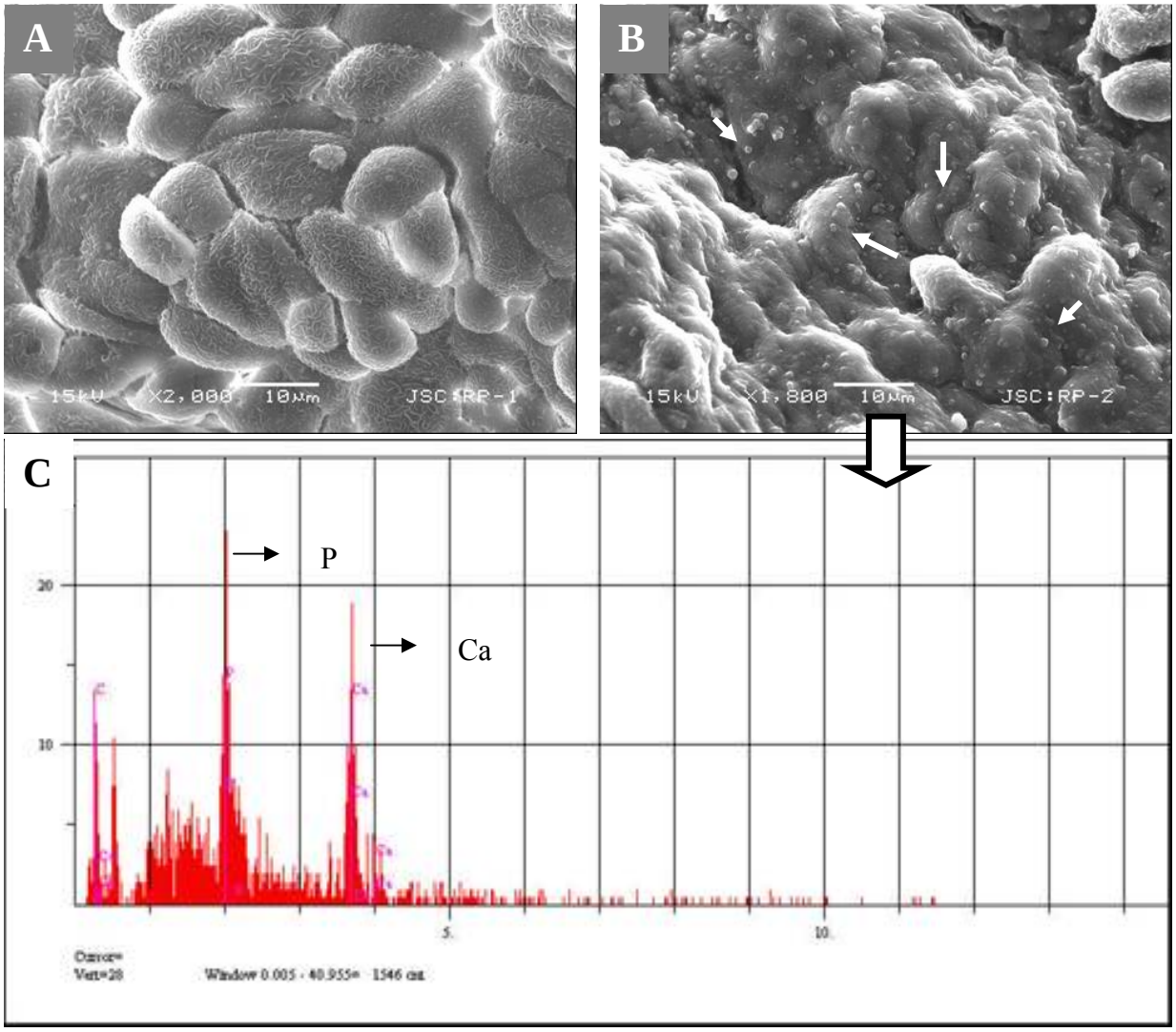

Figure 5. SEM analysis of renal papilla. A, Renall cells with no plaques. B, renal cells with plaque formations showing bumpy surface. White arrows show the spherical apatite formations on cells. C, EDS analysis of the one representative apatite sphere on the cells shown in B.

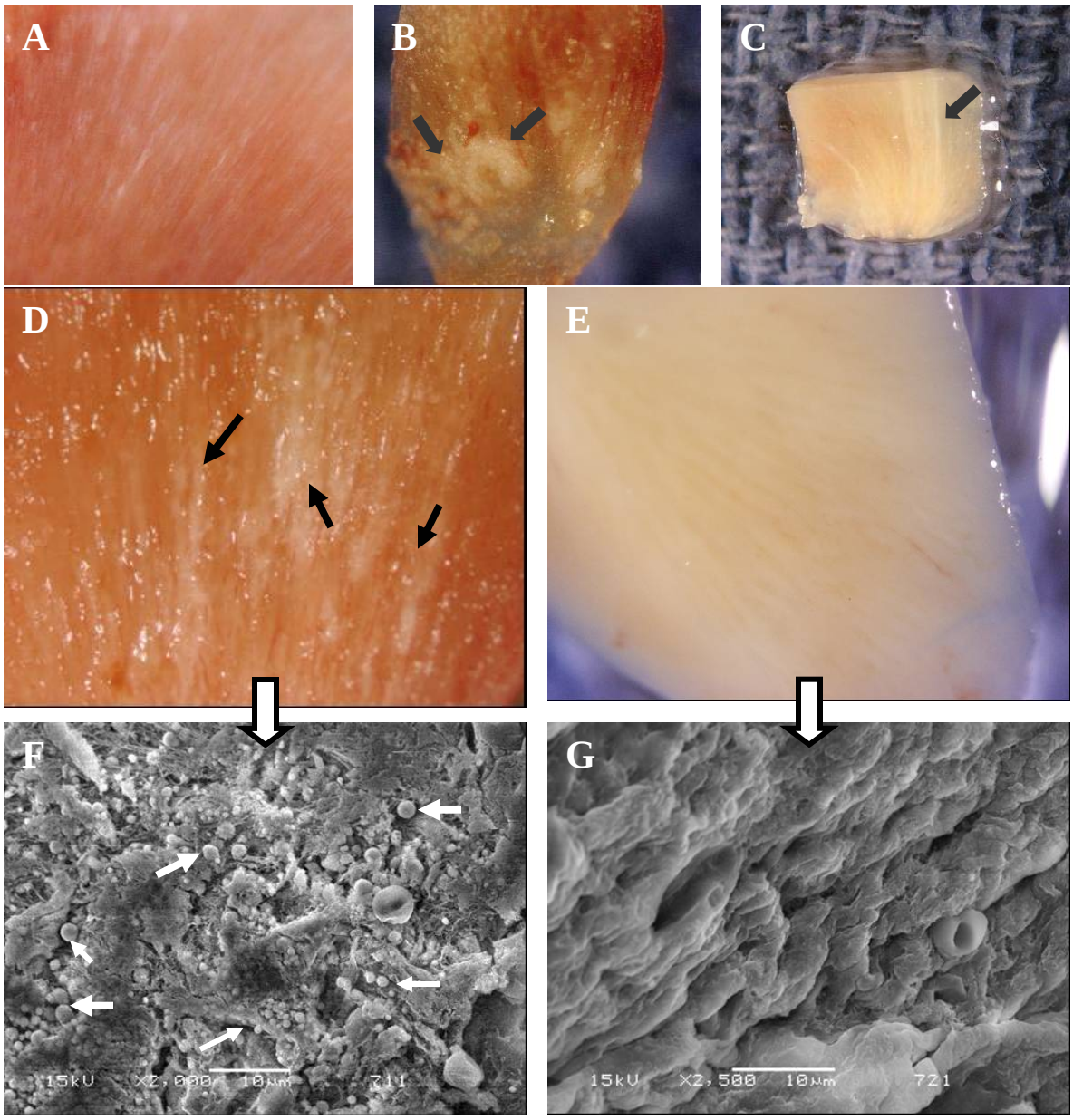

Figure 6. Images from Randall's plaques. (A) Tiny calcifications at the tip of the renal papilla. (B) Relatively large calcified plaques. (C) A cross section through the renal papilla, showing sub-epithelial calcifications running deep into the renal medulla. A closer images of renal papilla tissue with (D) and without eye-visible plaque formations (E). (F) and G are SEM images of the tissues shown at (D) and (E) respectively. Black arrows show streaks of plaques on the tissue, white small arrows show the apatite spheres on the tissue. Bars: F and G are 10μm.

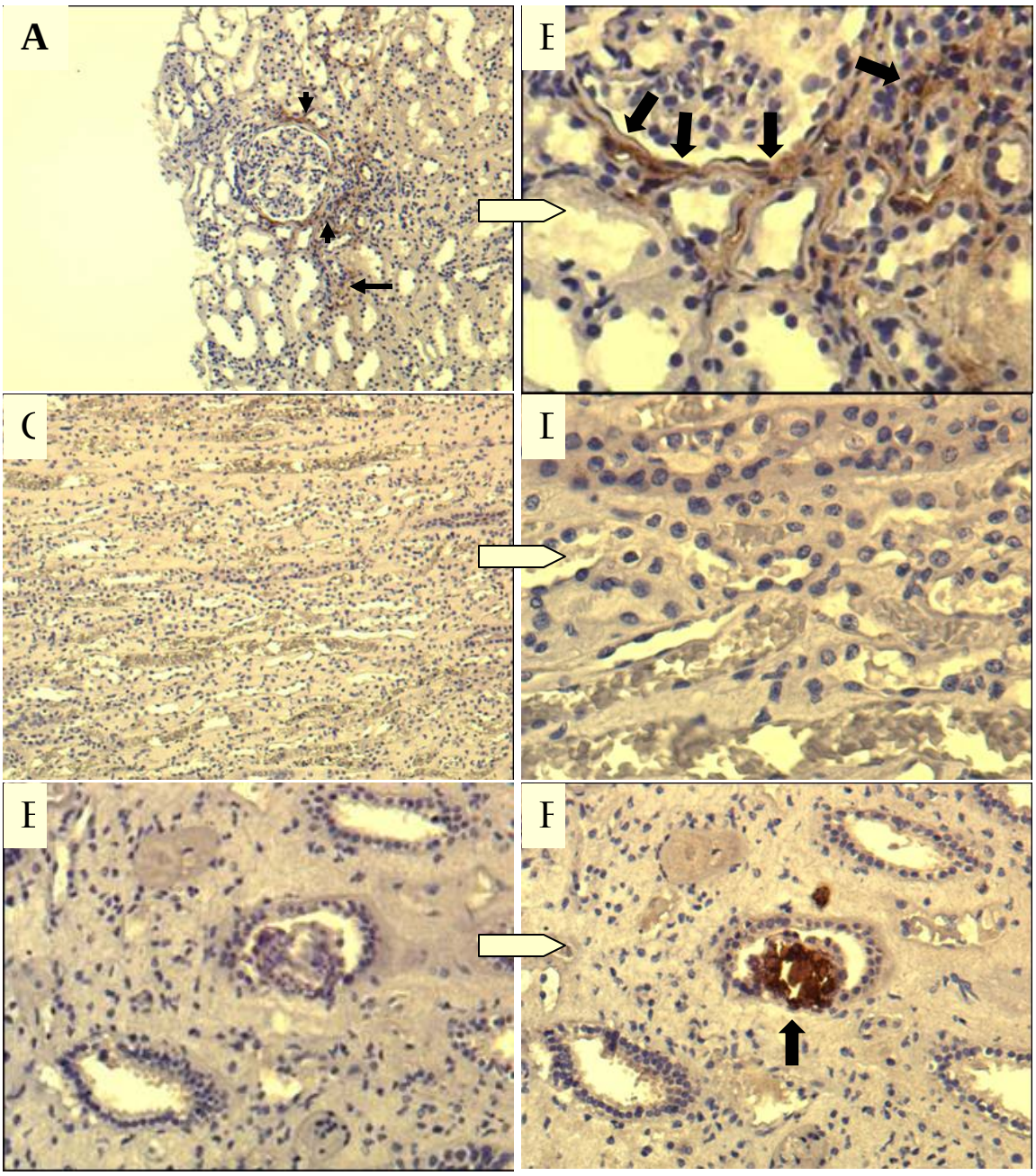

Figure 7. Immunohistochemical (IHS) staining of paraffin embedded renal papilla tissue by using anti-CNP monoclonal antibody. Brown color shown by black arrows indicates positive signal (existence of CNP antigen) in the tissue. The images shown at A (100X) and B (400X) are from IHS-positive tissue. C (100X) and D (400X) are from IHS-negative tissue, E and F (200X) are consecutive sections from a positive tissue. E is stained by omitting the monoclonal antibody, showing no positive signal whereas in F positively stained in one of the collecting ducts.